nature medicine

HIV persistence in tissue macrophages of humanized myeloid-only mice during antiretroviral therapy

Jenna B Honeycutt[1], William O Thayer[1], Caroline E Baker[1], Ruy M Ribeiro[2], Steven M Lada[3], Youfang Cao[2], Rachel A Cleary[1], Michael G Hudgens[4], Douglas D Richman[3,5,6] & J Victor Garcia[1]

© 2017 Nature America, Inc., part of Springer Nature. All rights reserved.

Despite years of fully suppressive antiretroviral therapy (ART), HIV persists in its hosts and is never eradicated. One major barrier to eradication is that the virus infects multiple cell types that may individually contribute to HIV persistence. Tissue macrophages are critical contributors to HIV pathogenesis[1–3]; however, their specific role in HIV persistence during long-term suppressive ART has not been established[4–6]. Using humanized myeloid-only mice (MoM), we demonstrate that HIV infection of tissue macrophages is rapidly suppressed by ART, as reflected by a rapid drop in plasma viral load and a dramatic decrease in the levels of cell-associated viral RNA and DNA. No viral rebound was observed in the plasma of 67% of the ART-treated animals at 7 weeks after ART interruption, and no replication-competent virus was rescued from the tissue macrophages obtained from these animals. In contrast, in a subset of animals (~33%), a delayed viral rebound was observed that is consistent with the establishment of persistent infection in tissue macrophages. These observations represent the first direct evidence, to our knowledge, of HIV persistence in tissue macrophages *in vivo*.

Humanized bone marrow, liver, thymus (BLT) mice are reconstituted with human T cells and macrophages, both of which are targets for HIV infection *in vivo*[7–11]. Use of HIV-infected mice previously reconstituted with human macrophages and T cells permits assessment of the effect of ART on tissue macrophages in the presence of T cells, while allowing for interactions between the two cell types. We infected BLT mice (n = 18) with macrophage-tropic viruses (HIV-1_{CH040} or HIV-$1_{CH040\text{-}4013env}$)[7] and monitored plasma viremia longitudinally (**Fig. 1a** and **Supplementary Table 1**). Thirteen mice at 5 weeks after infection were treated once daily with triple-combination ART, in which three antiretroviral drugs were used[12–14]. Within 2 weeks of ART initiation, we observed a significant decrease in the plasma viremia of treated (black line) versus untreated (gray line) mice (**Fig. 1a**; Mann–Whitney test). This corresponded to an average 1.3-log reduction in plasma viral RNA after 1 week of treatment (**Fig. 1b**). We used the change in viral load after ART initiation to estimate the half-life of productively infected cells in BLT mice, which was approximately 2.4 d (**Fig. 1c**), similar to the previous estimate of ~2 d in humans[15–17].

To address the effect of ART specifically on infected tissue macrophages, cells were pooled from the spleen, liver, lung, and bone marrow of individual ART-treated or untreated BLT mice. A stepwise magnetic cell sorting strategy was used to isolate T cells and macrophages (**Fig. 1d** and **Supplementary Fig. 1a–c**)[7]. We were able to detect cell-associated viral DNA (**Fig. 1e**) and RNA (**Fig. 1f**) in the purified T cell fractions of untreated mice. In ART-treated mice, the levels of viral DNA and RNA in T cells were reduced but readily detectable (**Fig. 1e**,**f**). In the purified macrophage fraction, we were able to readily detect viral DNA and RNA in untreated mice; however, the levels of viral DNA and RNA in tissue macrophages from ART-treated mice were below our level of detection using real-time PCR assays (**Fig. 1e**,**f**). We then conducted structured-treatment-interruption studies to assess the presence of persistently infected cells containing replication-competent virus (**Fig. 1g**,**h**)[12]. In all cases, HIV rebound was observed by 2 weeks after therapy interruption, which corresponds to a time to rebound within the range observed for patients with HIV[18]. Considering the absence of detectable viral RNA and DNA in macrophages isolated from ART-treated BLT mice, the rapid rebound observed ostensibly results from virus present in T cells.

MoM are generated by transplanting human CD34$^+$ hematopoietic stem cells into NOD/SCID mice, which are unable to support human T cell development[19]. MoM are systemically reconstituted with human myeloid and B cells, but not human T cells (**Supplementary Fig. 2**)[7].We have previously shown that MoM are susceptible to HIV infection and can efficiently sustain systemic HIV replication over several months[7]. MoM were used to avoid the confounding complications of having an excess of T cells present during the evaluation of HIV persistence in macrophages. We infected MoM (n = 14) with the same macrophage-tropic HIV isolates used for the BLT mice in **Figure 1** (**Supplementary Table 1**) and monitored infection over time in the absence (n = 6) or presence (n = 8) of ART (**Supplementary Fig. 3**). In all treated MoM, we noted a rapid and significant drop in plasma

[1]Division of Infectious Diseases, Center for AIDS Research, University of North Carolina, School of Medicine, Chapel Hill, North Carolina, USA. [2]Theoretical Division, Los Alamos National Laboratory, Los Alamos, New Mexico, USA. [3]Veterans Affairs, San Diego Healthcare System, San Diego, California, USA. [4]Department of Biostatistics, University of North Carolina, Chapel Hill, North Carolina, USA. [5]Department of Medicine, University of California, San Diego, San Diego, California, USA. [6]Department of Pathology, University of California, San Diego, San Diego, California, USA. Correspondence should be addressed to J.V.G. (victor_garcia@med.unc.edu).

Received 10 January; accepted 13 March; published online 17 April 2017; doi:10.1038/nm.4319

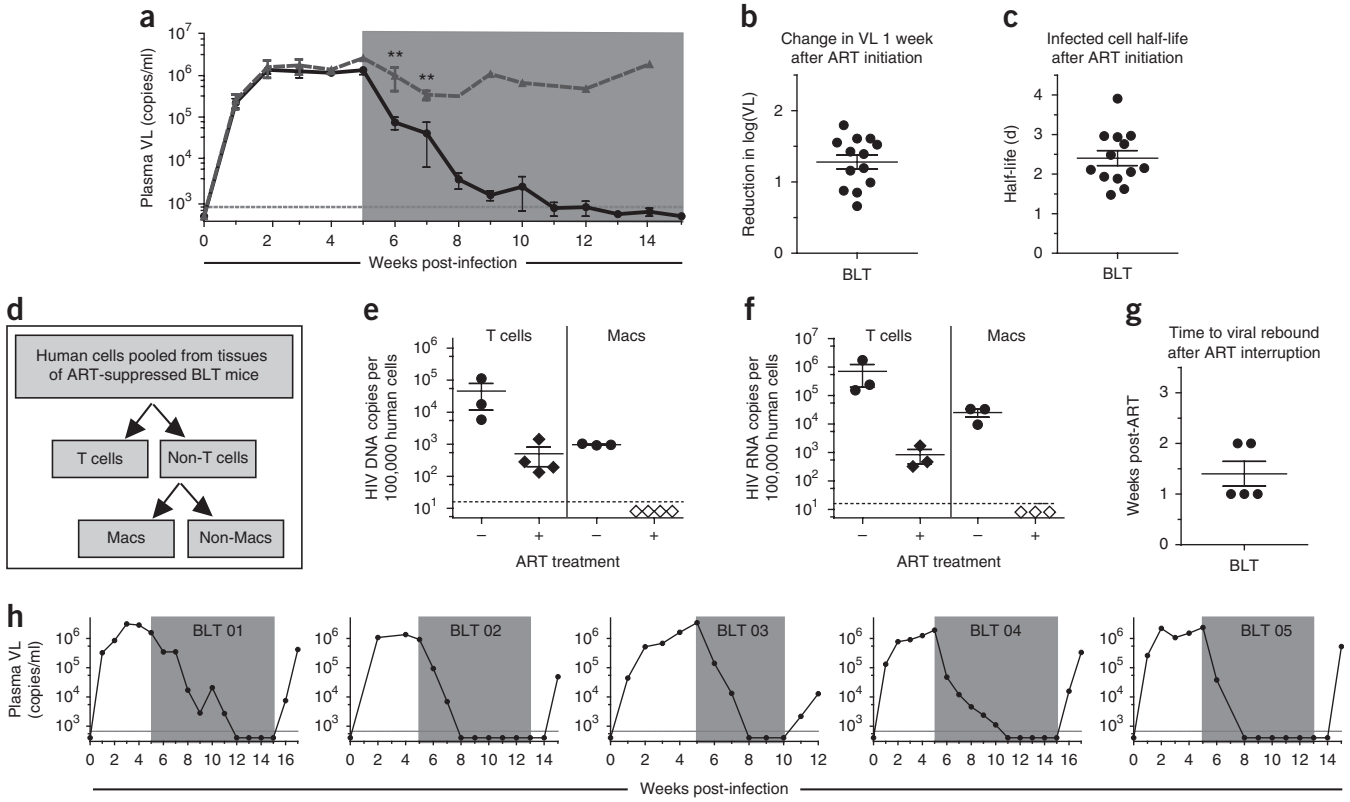

Figure 1 Viral suppression, persistence, and rebound induced by structured ART interruption in BLT mice. (**a**) Plasma viral load (VL) was monitored over time in HIV-infected ART-treated ($n = 13$; solid black line) and untreated ($n = 5$; dashed gray line) BLT mice. Each point represents mean ± s.e.m. The time of exposure to ART for the treated animals is indicated with a shaded gray box. A Mann–Whitney test was used to compare the plasma viral loads of ART-treated and untreated mice at 1 and 2 weeks following ART initiation ($P = 0.0049$ and $P = 0.0080$, respectively); $^{**}P < 0.01$. (**b**) The reduction in $\log_{10}$ plasma viral load was calculated 1 week after ART initiation for each treated BLT mouse ($n = 13$). (**c**) The half-life of productively infected cells was estimated from the change in viral load during ART ($n = 13$). (**d**) Schematic for the magnetic sorting and purification of human T cells and macrophages from tissues obtained from infected animals. Human T cells ($CD3^+$) and non-T cells were separated from pooled tissue cells of individual ART-treated BLT mice ($n = 4$). Macrophages (Macs) were then isolated from the non–T cell fraction. (**e**,**f**) Analysis of HIV DNA (**e**) and RNA (**f**) levels was performed by real-time PCR using purified cells isolated from ART-treated ($n = 4$) and untreated ($n = 3$) BLT mice. HIV DNA and RNA levels were normalized and are reported per 100,000 human cells. Samples with values below the level of detection are represented by open diamonds in **e** and **f** and are shown at the average lower limit of detection (dashed line). (**g**) Time to viral rebound after ART interruption in BLT mice ($n = 5$). (**h**) Viral rebound was observed 1–2 weeks after ART interruption in all BLT mice. The time of exposure to ART for each treated animal is indicated with a shaded gray box. For **b**, **c**, and **e**–**g**, data are represented as mean ± s.e.m.

viremia below the limit of detection relative to untreated MoM (**Fig. 2a**; Mann–Whitney test). After 1 week of ART, this drop corresponded to an average 1.8-log reduction in plasma viral RNA levels (**Fig. 2b**). This reduction in plasma viral RNA levels was significantly larger than the reduction observed in BLT mice (**Fig. 1b**; Mann–Whitney test, $P = 0.039$). Using the change in viral load after ART initiation, we estimated the half-life of productively infected macrophages in MoM to be 1.05 d (**Fig. 2c**), which is notably shorter than the estimated half-life of infected T cells in humans and BLT mice (**Fig. 1c**; Mann–Whitney test, $P = 0.0002$)[15–17]. Although the half-life of HIV-infected macrophages in MoM is shorter than that previously estimated for macrophages in macaques infected with simian/human immunodeficiency virus (SHIV)[20], our results are consistent with the more recent estimate of 1.33 d in $CD4^+$ T cell–depleted macaques infected with simian immunodeficiency virus (SIV) on combination ART[21].

We determined the levels of cell-associated viral DNA and RNA in tissue macrophages isolated from the liver, lung, spleen, and bone marrow of untreated or ART-treated MoM (**Supplementary Table 1**). Notably, the levels of viral DNA in 18 of 24 samples from 6 ART-treated MoM were below the level of detection (empty boxes in **Fig. 2d**; log-rank test, $P = 0.0003$, $P = 0.002$, $P = 0.007$, and $P = 0.0003$ for liver, lung, spleen, and bone marrow, respectively). Using an ultrasensitive quantitative droplet PCR technique, we demonstrated that HIV was integrated into the genome in a portion of the HIV DNA samples in the ART-treated group (a total of four samples were analyzed) and that the levels of integrated HIV DNA were significantly lower in treated animals (**Supplementary Fig. 3c**). In accordance with this significant decrease in viral DNA levels, the viral RNA levels of 11 of the 15 samples analyzed were also below the level of detection in 5 ART-treated MoM (empty boxes in **Fig. 2e**; log-rank test, $P = 0.005$, $P = 0.008$, $P = 0.008$, and $P = 0.001$ for liver, lung, spleen, and bone marrow, respectively). This difference in HIV DNA and RNA levels between treated and untreated mice did not result from a loss of macrophages in the tissues of treated mice (**Fig. 2f**; Mann–Whitney test, $P > 0.05$ for all tissue types). The limited detection of viral DNA and RNA from ART-treated MoM samples is consistent with our data obtained from purified macrophages isolated from the tissues of ART-treated BLT mice (**Fig. 1e**,**f**).

To determine whether HIV persists in infected tissue macrophages and can re-establish persistent infection after ART treatment, we

© 2017 Nature America, Inc., part of Springer Nature. All rights reserved.

discontinued therapy in HIV-infected MoM with HIV suppressed on ART (**Supplementary Table 1**). In sharp contrast with what was observed in BLT mice, where viral rebound was observed within 2 weeks of therapy discontinuation in all animals (n = 5), no viral rebound was observed in 6 of 9 MoM in an extended timeframe (greater than 7 weeks) (**Fig. 3a**). Upon further examination of tissue macrophages isolated from MoM in which no HIV rebound was observed, we detected no viral DNA or RNA (**Table 1**). To determine whether

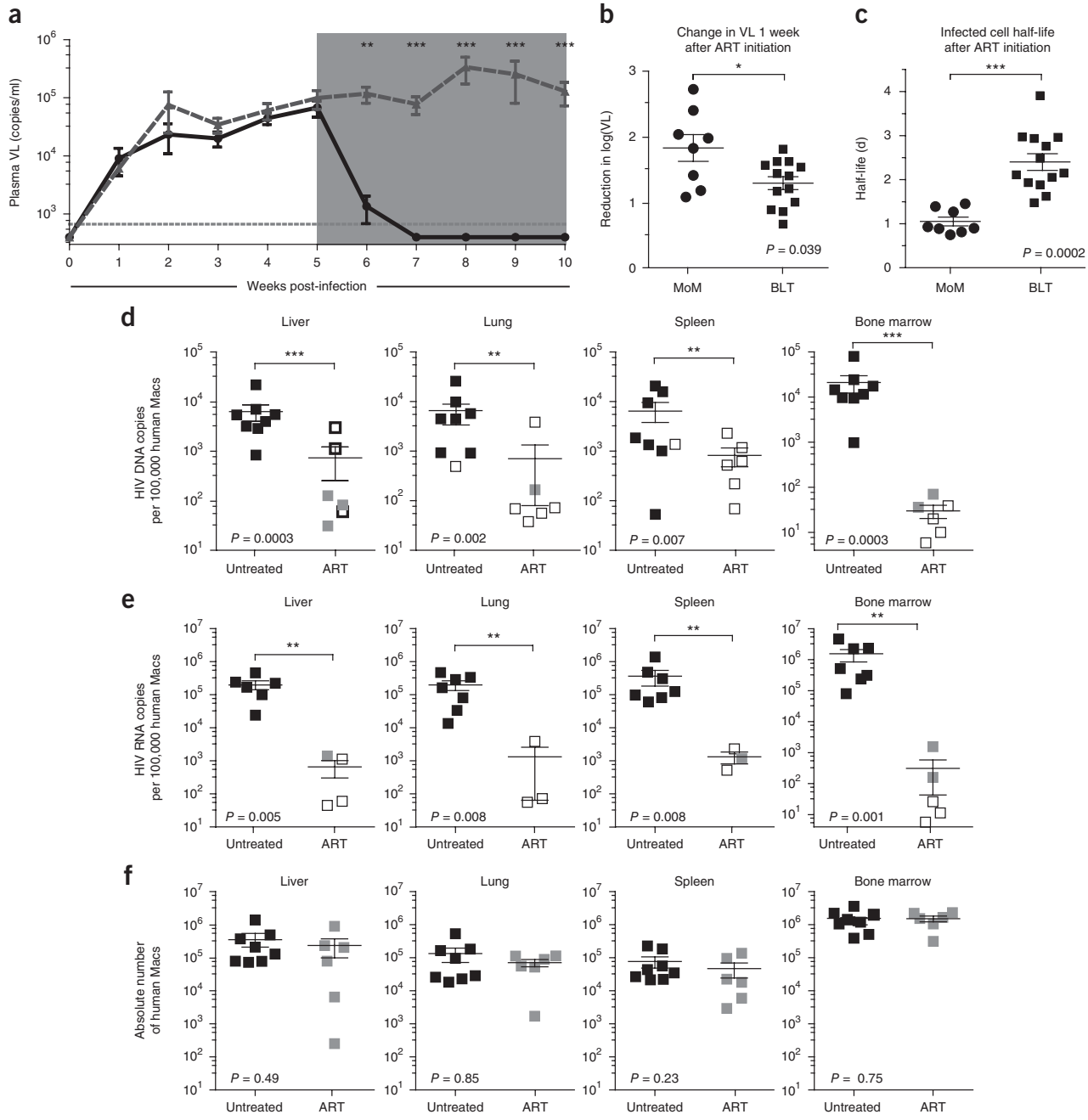

Figure 2 ART rapidly suppresses viral replication in MoM. (**a**) Longitudinal analysis of the plasma viral load in HIV-infected ART-treated (n = 8; solid black line) and untreated (n = 6; dashed gray line) MoM. Each point represents mean ± s.e.m. A Mann–Whitney test was used to compare the plasma viral loads of treated and untreated mice at 1–5 weeks following ART initiation (P = 0.0019, P = 0.0008, P = 0.0008, P = 0.0011, and P = 0.0017, respectively). The time of exposure to ART for treated animals is indicated with a shaded gray box. (**b**) The reduction in $\log_{10}$ plasma viral load was calculated 1 week after ART initiation for each treated MoM (n = 8). (**c**) The half-life of productively infected cells was estimated from the change in viral load during ART (n = 8). A Mann–Whitney test was used to compare MoM and BLT mice in **b** and **c**. (**d**,**e**) Cell-associated HIV DNA (**d**) and RNA (**e**) levels were measured in the liver, lung, spleen, and bone marrow of ART-treated (n = 6; gray squares) and untreated (n = 8; black squares) MoM. Undetectable samples are represented by an empty black box shown at the limit of detection for that sample (dependent on the number of cells available for analysis). Viral DNA and RNA levels were normalized per 100,000 human macrophages and compared between treated and untreated mice. A log-rank test was used to account for censoring due to the limits of detection in **d** and **e**. (**f**) There was no difference in the total numbers of human macrophages present in the tissues of ART-treated and untreated MoM (P > 0.05 for all tissue types, Mann–Whitney test). In **b**–**f**, horizontal lines represent mean ± s.e.m. P values for **a**–**e** are represented as follows: *P < 0.05, **P < 0.01, ***P < 0.001.

© 2017 Nature America, Inc., part of Springer Nature. All rights reserved.

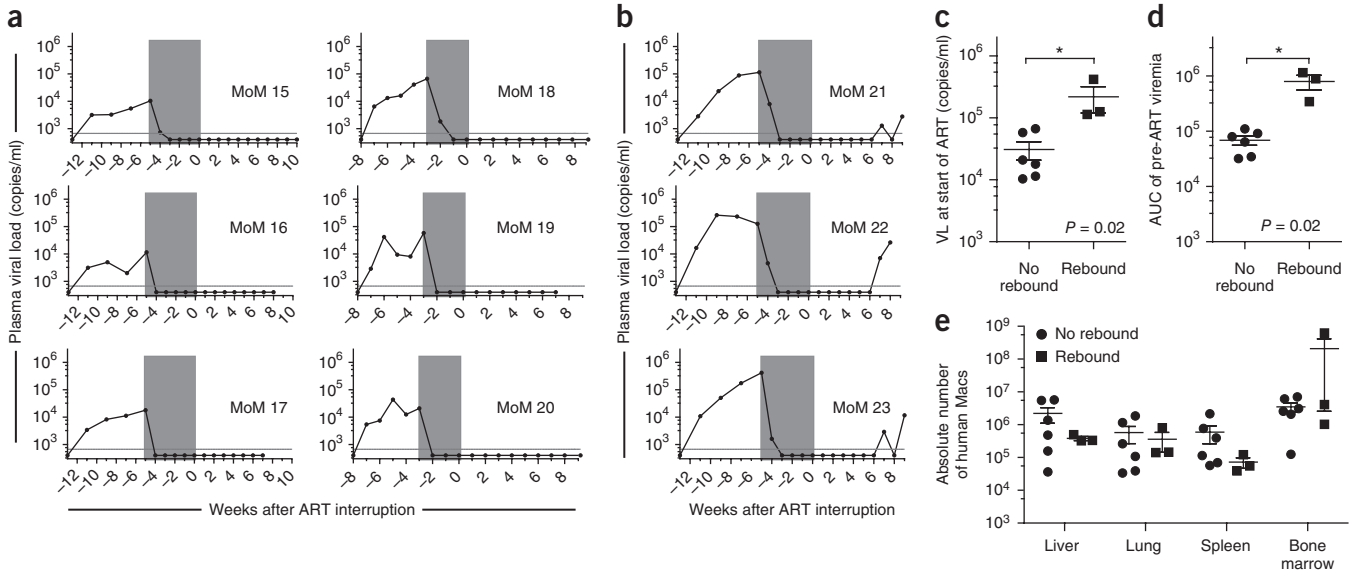

Figure 3 HIV persistence in tissue macrophages during ART. Viral rebound was absent in most infected MoM after structured ART interruption. (**a**,**b**) Viral load in no-rebound ($n = 6$) (**a**) and rebound ($n = 3$) (**b**) mice. The time of exposure to ART for each treated animal is indicated with a shaded gray box. (**c**,**d**) Higher plasma viral load at the start of treatment (**c**) and higher total viral burden (as demonstrated by area under the curve (AUC) analysis of pre-ART viremia) (**d**) were associated with viral rebound after ART interruption. (**e**) The total numbers of human macrophages in the tissues of MoM were similar for mice in which viral rebound was absent (**a**) and observed (**b**) ($P > 0.05$). Mann–Whitney tests were used to compare mice in **c**–**e**. For **c**–**e**, data are represented as mean ± s.e.m. $^*P < 0.05$.

persistent, replication-competent virus was present in tissue macrophages isolated from ART-treated MoM in which no rebound was observed, we applied outgrowth assays similar to those previously used in macaques to either quantify virus from infected macrophages[22] or establish SIV eradication after vaccination with an hCMV-based vector[23,24]. For this purpose, cells obtained from the MoM in which viral rebound was not observed were directly injected into BLT humanized mice, as we have previously described[7], or were co-cultured with $CD8^+$-depleted activated allogeneic $CD4^+$ T cells[7,25–27]. Plasma or tissue culture supernatants were then monitored for the presence of viral outgrowth; however, no replication-competent virus was rescued from any of the five MoM that were analyzed (**Table 1**). Fewer total numbers of cells were isolated from MoM 19, precluding additional outgrowth analysis for this mouse.

In plasma from three of the MoM, we observed viral rebound 7 weeks after ART interruption (**Fig. 3b**). We confirmed the absence of human T cells in the tissues of 'rebound' MoM (**Supplementary Fig. 4**). We demonstrated the replication competence of the rebound virus (from MoM 23) to infect both T cells and macrophages using the same outgrowth assays performed on the 'no rebound' MoM (**Supplementary Fig. 5** and **Supplementary Table 2**). Additionally, HIV *env* was sequenced from the plasma of rebound MoM and compared to the sequence of the original virus used for infection. No mutations were found in MoM 22. In MoM 21 and 23, a point mutation was present, resulting in single-amino-acid changes (I262L and I107S, respectively) in the env sequence (GenBank accession numbers KX825880 and KX825881). In MoM 23, the mutation was present in ~50% of the bulk sequence. A *post hoc* comparison of mice with and without HIV rebound demonstrated a higher pre-ART viral load (**Fig. 3c**) and a larger total pre-ART viral burden (as demonstrated by the area under the curve for pre-ART viremia; **Fig. 3d**) in the rebound mice (Mann–Whitney test, $P = 0.02$). No differences were noted between rebound and no-rebound mice in the overall levels of human cells in the blood (Mann–Whitney test, $P = 0.381$) or the number of tissue macrophages (**Fig. 3e**; Mann–Whitney test, $P > 0.05$). This suggests that, under our experimental conditions, the lack of rebound observed in six of the nine mice was not simply due

Table 1 Absence of replication-competent virus in tissues of MoM without plasma viral rebound after ART interruption

					Viral outgrowth analysis performed on tissue cells		
Mouse number	% human	Virus	HIV DNA	HIV RNA	Observation	Method	No. cells
MoM 15	42	CH040	Below LOD	ND	No outgrowth	*In vitro*	63×10^6
MoM 16	63	CH040	Below LOD	ND	No outgrowth	*In vitro*	44×10^6
MoM 17	49	CH040	Below LOD	ND	No outgrowth	*In vitro*	30×10^6
MoM 18	28	CH040	Below LOD	Below LOD	No outgrowth	*In vivo*	4×10^6
MoM 19	8	CH040	Below LOD	ND	ND	ND	ND
MoM 20	16	CH040	Below LOD	Below LOD	No outgrowth	*In vivo*	4×10^6

HIV DNA and RNA analysis and *in vivo* or *in vitro* viral outgrowth assays were performed with cells isolated from ART-treated MoM in which plasma viral rebound was not observed. The tissues analyzed for all mice included the spleen, liver, lung, brain, and bone marrow. In MoM 18–20, the gastrointestinal and female reproductive tracts were also analyzed for the presence of HIV DNA. For the viral outgrowth assays, cells isolated from the tissues of MoM were (i) cultured with activated allogeneic $CD4^+$ T cells and culture supernatants were tested for the presence of cell-free HIV RNA by real-time PCR analysis (*in vitro* method) or (ii) injected into BLT mice and plasma viral load was monitored over time to determine the presence or absence of HIV infection in recipient mice (*in vivo* method). The total number of cells used for outgrowth analysis is indicated (no. cells). LOD, limit of detection; ND, not determined.

© 2017 Nature America, Inc., part of Springer Nature. All rights reserved.

to insufficient numbers of human-derived tissue macrophages, but was due to the absence of productively infected cells capable of restarting the infection. We then used these data to model the likely persistence of HIV-infected macrophages under ART in view of their half-life. Our estimate of approximately 1 d for the half-life of infected macrophages indicates that half of all infected macrophages are lost every day. Therefore, the number of productively infected macrophages under ART would be expected to decay to about 1% after 1 week and to less than 0.00001% of the initial value during the 5 weeks of treatment. The fact that viral rebound was observed 7 weeks after therapy interruption (and was absent in most of the treated MoM) is consistent with the existence of a small population of infected tissue macrophages that persist despite ART, especially when pretreatment viral burden is greatest.

As in any study involving the use of a model system, there are some caveats to this analysis. First, the strain of immunodeficient mice used to generate MoM (NOD/SCID mice) develop spontaneous thymic lymphomas, resulting in a relatively short lifespan (9–14 months)[28]. This limitation prevented us from extending our observations of infected MoM after interruption of ART for longer periods of time. Therefore, outgrowth assays were used to confirm the absence of cells containing replication-competent virus. Second, certain interactions between T cells and macrophages may be critical for persistent HIV infection; therefore, our results in MoM may underestimate the frequency of viral rebound from macrophages. However, this is unlikely to be the case, as the disappearance of infected macrophages was noted in both ART-treated, HIV-infected BLT mice and MoM, suggesting that the presence of human T cells is not critical for HIV persistence in human macrophages.

Antiretroviral therapy alone is not sufficient to eradicate HIV from the body. Hill *et al.* indicate that reductions of 2–3 logs in the number of latently infected cells are needed to delay rebound for the time reported herein for MoM[29]. The delay in rebound observed in MoM is greater than that reported for patients initiating ART during the chronic phase of infection[30] and for patients with an ultralow HIV reservoir[18]. Our results indicate that HIV-infected tissue macrophages have a short half-life and that ART alone can significantly reduce the levels of infected tissue macrophages, further demonstrating the critical contribution of T cells to the viral reservoir. Given the short half-life of infected macrophages during ART treatment, it is possible that, under extended ART treatment, no viral rebound from macrophages would be observed in MoM. In patients in whom viral rebound occurs after a long period following ART interruption, the cellular identity and location within the tissue of the HIV reservoir is unknown[31,32]. However, the fact that viral rebound can be observed in 33% of the infected, virally suppressed mice suggests that macrophages may represent a persistent viral reservoir for HIV. Specialized, long-lived macrophages, such as microglia, are thought to persist in the central nervous system (CNS) for long periods of time despite infection[33,34] and could thus contribute to viral persistence over time. Therefore, our results show that productively infected tissue macrophages can persist in the host despite effective treatment and can re-establish productive infection after structured treatment interruption.

METHODS

Methods, including statements of data availability and any associated accession codes and references, are available in the online version of the paper.

Note: Any Supplementary Information and Source Data files are available in the online version of the paper.

ACKNOWLEDGMENTS

We thank N. Archin (University of North Carolina at Chapel Hill) for providing the CD8$^+$-depleted feeder cells for *in vitro* viral outgrowth analysis; J. Kappes and C. Ochsenbauer (University of Alabama at Birmingham) for providing CH040 (11740) via the AIDS Research and Reference Reagent Program; R. Swanstrom (University of North Carolina at Chapel Hill) for providing 4013-env for use in our studies; J. Clements, R. Siliciano, and D. Margolis for their intellectual input in these studies; M. Cohen, B. Haynes, S. Lemon, A. Wahl, and M. Kovarova for their comments and suggestions regarding this manuscript; and former and current members of the Garcia laboratory and the husbandry technicians at the UNC Division of Laboratory Animal Medicine for their assistance. J.V.G. was supported by grants from the National Institute of Mental Health (MH-108179) and the National Institute of Allergy and Infectious Diseases (NIAID) (AI-111899) and by the UNC CFAR (P30 AI050410). Research reported in this publication was also supported by CARE, a Martin Delaney Collaboratory, the National Institute of Allergy and Infectious Diseases (NIAID), the National Institute of Neurological Disorders and Stroke (NINDS), the National Institute on Drug Abuse (NIDA), and the National Institute of Mental Health (NIMH) of the National Institutes of Health, grant number 1UM1AI126619-01 (J.V.G. and D.D.R.). The content is solely the responsibility of the authors and does not necessarily represent the official views of the National Institutes of Health. J.B.H. was supported in part by the Virology Training Grant (T32 AI-007419). R.M.R. was supported by the NIAID (R01 AI-104373). D.D.R. was also supported by the BEAT-HIV Delaney Collaboration (1UM1AI126620), the UCSD CFAR (AI306214), the Department of Veterans Affairs, and the James B. Pendleton Charitable Trust. The funders had no part in study design, data collection or analysis, decision to publish, or preparation of the manuscript.

AUTHOR CONTRIBUTIONS

J.B.H. provided the experimental design, collected and processed blood and tissue samples from mice, prepared viral stocks, performed viral inoculations, administered ART, and performed flow cytometric analyses. W.O.T. processed blood and tissue samples from mice, prepared the injectable ART formulation, and administered ART. C.E.B. provided RNA and DNA analysis, prepared the injectable ART formulation, and processed tissue samples. R.A.C. performed immunohistochemical analysis of tissues. S.M.L. and D.D.R. performed the integrated DNA analysis and analyzed the results. J.B.H., R.M.R., Y.C., and M.G.H. analyzed the data and wrote the manuscript. J.V.G. conceived the study, designed and coordinated the study, and wrote the manuscript.

COMPETING FINANCIAL INTERESTS

The authors declare no competing financial interests.

Reprints and permissions information is available online at http://www.nature.com/reprints/index.html.

1. Kumar, A. & Herbein, G. The macrophage: a therapeutic target in HIV-1 infection. *Mol. Cell. Ther.* **2**, 10 (2014).
2. Koppensteiner, H., Brack-Werner, R. & Schindler, M. Macrophages and their relevance in human immunodeficiency virus type I infection. *Retrovirology* **9**, 82 (2012).
3. Campbell, J.H., Hearps, A.C., Martin, G.E., Williams, K.C. & Crowe, S.M. The importance of monocytes and macrophages in HIV pathogenesis, treatment, and cure. *AIDS* **28**, 2175–2187 (2014).
4. Sattentau, Q.J. & Stevenson, M. Macrophages and HIV-1: an unhealthy constellation. *Cell Host Microbe* **19**, 304–310 (2016).
5. Collman, R.G., Perno, C.F., Crowe, S.M., Stevenson, M. & Montaner, L.J. HIV and cells of macrophage/dendritic lineage and other non–T cell reservoirs: new answers yield new questions. *J. Leukoc. Biol.* **74**, 631–634 (2003).
6. Gavegnano, C. & Schinazi, R.F. Antiretroviral therapy in macrophages: implication for HIV eradication. *Antivir. Chem. Chemother.* **20**, 63–78 (2009).
7. Honeycutt, J.B. *et al.* Macrophages sustain HIV replication *in vivo* independently of T cells. *J. Clin. Invest.* **126**, 1353–1366 (2016).
8. Denton, P.W. *et al.* Systemic administration of antiretrovirals prior to exposure prevents rectal and intravenous HIV-1 transmission in humanized BLT mice. *PLoS One* **5**, e8829 (2010).
9. Wahl, A. *et al.* Human breast milk and antiretrovirals dramatically reduce oral HIV-1 transmission in BLT humanized mice. *PLoS Pathog.* **8**, e1002732 (2012).
10. Olesen, R., Wahl, A., Denton, P.W. & Garcia, J.V. Immune reconstitution of the female reproductive tract of humanized BLT mice and their susceptibility to human immunodeficiency virus infection. *J. Reprod. Immunol.* **88**, 195–203 (2011).
11. Melkus, M.W. *et al.* Humanized mice mount specific adaptive and innate immune responses to EBV and TSST-1. *Nat. Med.* **12**, 1316–1322 (2006).
12. Denton, P.W. *et al.* Generation of HIV latency in humanized BLT mice. *J. Virol.* **86**, 630–634 (2012).
13. Denton, P.W. *et al.* Targeted cytotoxic therapy kills persisting HIV infected cells during ART. *PLoS Pathog.* **10**, e1003872 (2014).

© 2017 Nature America, Inc., part of Springer Nature. All rights reserved.

14. Thompson, M.A. *et al.* Antiretroviral treatment of adult HIV infection: 2012 recommendations of the International Antiviral Society–USA panel. *J. Am. Med. Assoc.* **308**, 387–402 (2012).
15. Perelson, A.S., Neumann, A.U., Markowitz, M., Leonard, J.M. & Ho, D.D. HIV-1 dynamics *in vivo*: virion clearance rate, infected cell life-span, and viral generation time. *Science* **271**, 1582–1586 (1996).
16. Ho, D.D. *et al.* Rapid turnover of plasma virions and CD4 lymphocytes in HIV-1 infection. *Nature* **373**, 123–126 (1995).
17. Wei, X. *et al.* Viral dynamics in human immunodeficiency virus type 1 infection. *Nature* **373**, 117–122 (1995).
18. Calin, R. *et al.* Treatment interruption in chronically HIV-infected patients with an ultralow HIV reservoir. *AIDS* **30**, 761–769 (2016).
19. Shultz, L.D., Ishikawa, F. & Greiner, D.L. Humanized mice in translational biomedical research. *Nat. Rev. Immunol.* **7**, 118–130 (2007).
20. Igarashi, T. *et al.* Macrophage are the principal reservoir and sustain high virus loads in rhesus macaques after the depletion of CD4$^+$ T cells by a highly pathogenic simian immunodeficiency virus/HIV type 1 chimera (SHIV): implications for HIV-1 infections of humans. *Proc. Natl. Acad. Sci. USA* **98**, 658–663 (2001).
21. Micci, L. *et al.* CD4 depletion in SIV-infected macaques results in macrophage and microglia infection with rapid turnover of infected cells. *PLoS Pathog.* **10**, e1004467 (2014).
22. Avalos, C.R. *et al.* Quantitation of productively infected monocytes and macrophages of simian immunodeficiency virus–infected macaques. *J. Virol.* **90**, 5643–5656 (2016).
23. Hansen, S.G. *et al.* Profound early control of highly pathogenic SIV by an effector memory T-cell vaccine. *Nature* **473**, 523–527 (2011).
24. Hansen, S.G. *et al.* Immune clearance of highly pathogenic SIV infection. *Nature* **502**, 100–104 (2013).
25. Sung, J.A. *et al.* Expanded cytotoxic T-cell lymphocytes target the latent HIV reservoir. *J. Infect. Dis.* **212**, 258–263 (2015).
26. Archin, N.M. *et al.* Valproic acid without intensified antiviral therapy has limited impact on persistent HIV infection of resting CD4$^+$ T cells. *AIDS* **22**, 1131–1135 (2008).
27. Spina, C.A. *et al.* An in-depth comparison of latent HIV-1 reactivation in multiple cell model systems and resting CD4$^+$ T cells from aviremic patients. *PLoS Pathog.* **9**, e1003834 (2013).
28. Prochazka, M., Gaskins, H.R., Shultz, L.D. & Leiter, E.H. The nonobese diabetic *scid* mouse: model for spontaneous thymomagenesis associated with immunodeficiency. *Proc. Natl. Acad. Sci. USA* **89**, 3290–3294 (1992).
29. Hill, A.L. *et al.* Real-time predictions of reservoir size and rebound time during antiretroviral therapy interruption trials for HIV. *PLoS Pathog.* **12**, e1005535 (2016).
30. Steingrover, R. *et al.* HIV-1 viral rebound dynamics after a single treatment interruption depends on time of initiation of highly active antiretroviral therapy. *AIDS* **22**, 1583–1588 (2008).
31. Persaud, D. *et al.* Absence of detectable HIV-1 viremia after treatment cessation in an infant. *N. Engl. J. Med.* **369**, 1828–1835 (2013).
32. Henrich, T.J. *et al.* Long-term reduction in peripheral blood HIV type 1 reservoirs following reduced-intensity conditioning allogeneic stem cell transplantation. *J. Infect. Dis.* **207**, 1694–1702 (2013).
33. Nath, A. & Clements, J.E. Eradication of HIV from the brain: reasons for pause. *AIDS* **25**, 577–580 (2011).
34. Joseph, S.B., Arrildt, K.T., Sturdevant, C.B. & Swanstrom, R. HIV-1 target cells in the CNS. *J. Neurovirol.* **21**, 276–289 (2015).

© 2017 Nature America, Inc., part of Springer Nature. All rights reserved.

© 2017 Nature America, Inc., part of Springer Nature. All rights reserved.

ONLINE METHODS

Generation of humanized mice. Mice were created and monitored as previously described[7,12,13]. BLT mice were generated by implanting human thymus and liver tissue under the kidney capsule of sublethally irradiated NOD.Cg-*Prkdc*^{scid} *Il2rgtm1*^{Wjl}/SzJ mice (NSG; The Jackson Laboratory). BLT mice received 3.5×10^5 autologous CD34$^+$ hematopoietic stem cells. Humanized MoM were created by transplanting sublethally irradiated NOD.CB17-*Prkdc*^{scid}/J mice (NOD/SCID; The Jackson Laboratory) with approximately 1×10^6 cord blood or liver-derived CD34$^+$ hematopoietic stem cells. All animals were irradiated before stem cell transplantation (BLT mice, 200 rad; MoM, 250 rad). Mice were maintained in a specific-pathogen-free facility by the Division of Laboratory Animal Medicine at the University of North Carolina at Chapel Hill (UNC-CH) according to protocols approved by the Institutional Animal Care and Use Committee. A total of 36 female and 21 male animals were used, with an average age of 26 weeks (ranging from 13–48 weeks) at the start of the experiments.

HIV exposures. Stocks of CH040 and the chimeric virus CH040-4013 env were prepared and titered as previously described[7]. Briefly, virus-containing supernatants were prepared via transient transfection of 293T cells and were titered using TZM-bl cells (an indicator cell line). The TZM-bl cells were obtained through the NIH AIDS Reagent Program, Division of AIDS, NIAID, NIH (from J.C. Kappes, X. Wu and Tranzyme, Inc. (Cat. 8129); they were confirmed negative for bacteria, mycoplasma, and fungi. The chimeric virus was created by replacing *env* in CH040 (accession jn944905, 6,396–8,863 nt) with the corresponding restriction fragment from 4013 (accession jn562796). For the ART treatment experiments, humanized MoM and BLT mice were injected intravenously with 3.6×10^5 tissue culture infectious units (TCIU) of HIV. The untreated BLT mice in **Figure 1a** were exposed vaginally to 3.6×10^5 tissue culture infectious units (TCIU) of HIV. BLT mice were exposed 8–36 weeks after CD34$^+$ cell transplantation (mean 18.3 weeks), and MoM were exposed 8–26 weeks after CD34$^+$ cell transplantation (mean 16.7 weeks); there was no difference in the weeks after CD34$^+$ cell transplantation between MoM and BLT mice at the time of virus exposure (Mann–Whitney test, $P = 0.59$).

Monitoring of HIV infection in humanized mice. Peripheral blood was collected, and plasma was isolated by centrifugation. HIV infection was monitored in peripheral blood plasma with a one-step reverse transcriptase real-time PCR assay (ABI custom TaqMan assays-by-design) according to the manufacturer's instructions (with primers 5′-CATGTTTTCAGCATTATCAGAAGGA-3′ and 5′-TGCTTGATGTCCCCCCACT-3′; assay sensitivity of 668 RNA copies/ml). At necropsy, mononuclear cells (MNCs) were isolated from tissues and analyzed for the presence of viral RNA and DNA. For viral outgrowth analysis (**Table 1**), an *in vitro* or *ex vivo* outgrowth analysis was performed as done previously in MoM[7]. For the *in vitro* analysis, macrophages were plated and allowed to adhere. Within 24 h of plating, approximately 1 million allogenic, phytohemagglutinin (PHA)-stimulated feeder cells (CD8$^+$-depleted peripheral blood mononuclear cells from healthy human donors) were added to the cultures as targets for viral outgrowth (kindly provided by N. Archin, UNC-CH). After 10 d, culture supernatants were analyzed for the presence of viral RNA by real-time RT–PCR. For the *ex vivo* outgrowth analysis, cells were isolated from the tissues of ART-treated MoM, and ~4 million cells were injected intravenously into naive BLT mice. The plasma viral load was monitored for 4–8 weeks after injection, and tissues collected from BLT mice were analyzed for the presence of viral DNA at necropsy.

Integrated HIV DNA analysis. High-molecular-weight DNA (15 kb or greater in length) was separated by pulse-field gel electrophoresis with the automated BluePippin cassette system (S. Lada and D.D. Richman, personal communication). 30 µl of total DNA and 10 µl of loading buffer were pipetted onto one lane of a 0.75% agarose cassette. Using a high-pass protocol with a 15-kb cutoff and BluePippin S1 marker, high-molecular-weight DNA was purified and a total volume of 80 µl was collected. Afterwards, HIV Gag, HIV 2-LTR junction, and host cell RPP30 were assayed by droplet digital PCR (ddPCR). ddPCR analysis was performed as previously described[35].

Antiretroviral treatment of mice. For HIV treatment, we used a previously described combination of three drugs that we have shown are effective at suppressing viral load in T cell–only mice (ToM) and BLT mice[12,13,36]. Mice were administered daily intraperitoneal injections of emtricitabine (FTC; 211 mg per kg bodyweight), tenofovir disoproxil fumarate (TDF; 205 mg per kg bodyweight), and raltegravir (RAL; 56 mg per kg bodyweight) for 3–11 weeks, as indicated on individual graphs. HIV infection was monitored throughout ART via plasma viral load analysis as described above.

Tissue harvesting of humanized mice. To minimize the numbers of blood-derived monocytes in tissues collected from HIV-infected MoM and BLT mice, animals were transcardially perfused with ~20 ml of room-temperature PBS at necropsy. MNCs were isolated from the bone marrow, spleen, lung, and liver as previously described. Tissues were minced and/or digested and were filtered through a 70-µm strainer. Liver, lung, and brain samples were purified by Percoll density centrifugation. Red blood cells were lysed as needed (namely for the spleen, bone marrow, and liver tissues). MNCs were washed and counted via trypan blue exclusion.

Macrophage and T cell sorting. Total MNCs were isolated from the spleen, liver, lung, and bone marrow of HIV-infected BLT mice. Mouse cells were depleted using the EasySep Mouse/Human Chimera Isolation kit (Stem Cell Technologies, 19849) followed by positive magnetic selection for human CD3$^+$ T cells (Miltenyi, CD3 MicroBeads, 130-050-101). Next, negative magnetic selection for human monocytes and macrophages (Miltenyi, Pan Monocyte Isolation Kit, 130-096-537) was performed on the CD3$^-$ cell population to yield a purified macrophage population (<1% T cell contamination). Cell purity was verified using flow cytometric staining.

Flow cytometric analysis of humanized mice. All flow antibodies were purchased from BD Pharmingen. The antibody panel used to analyze cells isolated from humanized mice included antibodies directed against hCD45 (APC, 555485 or APC-Cy7, 557833), hCD3 (FITC, 555339), hCD19 (PE-Cy7, 557835), hCD33 (PE, 340679), hCD14 (FITC, 555397), hCD16 (PE-Cy7, 557744), hCCR5 (APC, 550856), and hCD11b (PE, 555388). All antibodies are routinely tested at BD Biosciences Pharmigen, and references for validation can be found on their website: http://www.bdbiosciences.com/us/home. Live cells were distinguished by their forward and side scatter profiles. Flow cytometry data were collected on a BD FACSCanto and analyzed with BD FACSDiva software (v.6.1.3).

Immunohistochemical analysis. Tissues for immunohistochemical analysis were collected from MoM and fixed in 4% paraformaldehyde for 24 h at 4 °C, embedded in paraffin, cut into 5-µm sections, and mounted onto poly (L-lysine)-coated glass slides. Following paraffin removal, antigen retrieval (DIVA Decloaker, Biocare Medical, DV2004.), and blocking of nonspecific Ig-binding sites (Background Sniper, Biocare Medical), tissue sections were stained with primary antibodies overnight at 4 °C and developed with a biotin-free horseradish peroxidase (HRP)-polymer system (MACH3 Mouse HRP-Polymer Detection, Biocare Medical). All tissue sections were then counterstained with hematoxylin. Primary antibodies directed against CD45 LCA (2B11 and PD7/26, Dako), CD3 (SP7, Thermo Scientific), CD20 (L26, Biocare Medical), and CD68 (KP1, Dako) were used to identify human cells in the spleen, liver, and lung. For comparison, tissue sections were stained with mouse IgG1k or IgG2a isotype control. Light microscopy images were acquired with a Nikon H550S microscope at 40×.

Sequencing of HIV-1 in MoM plasma. For sequence analysis of HIV-1 envelope, viral RNA was isolated from plasma from infected MoM using the QIAamp Viral RNA Mini kit (Qiagen). Viral cDNA was generated using Superscript III Reverse Transcriptase (Invitrogen) and amplified by nested PCR using the Expand High-Fidelity PCR System (Roche). The amplified region was a 1.2-kb region of HIV *env* (HIV_{CH040}, 6,426–7,702; $HIV_{CH040\text{-}4013env}$, 6,426–7,702). The primers used for CH040 *env* amplification included *env* outer forward primer (5′-CACCACTCTATTTTGTGCATCAGATG-3′), *env* outer reverse primer (5′-GCCCATAGTGCTTCCTGCTGC-3′), *env* inner

doi:10.1038/nm.4319

forward primer (5′-CACACATGCCTGTGTACCCACAGAC-3′), and *env* inner reverse primer (5′-CTCTTCTCTTTGCCTTGGTAGGTGC-3′). The primers used for CH040-4013env *env* amplification included *env* outer forward primer (5′-CACCACTCTATTTTGTGCATCAGATG-3′), *env* outer reverse primer (5′-GCCCATAGTGCTTCCTGCTGC-3′), *env* inner forward primer (5′-CAC ACATGCCTGTGTACCCACAGAC-3′), and *env* inner reverse primer (5′-CT CTTCTCTTTGCCTTGGTGGGTGC-3′). Amplified DNA was sequenced and aligned to the reference sequence for HIV-1_{CH040} or $HIV_{CH040\text{-}4013env}$ to determine whether nucleotide changes had occurred. FinchTV (Geospiza) was used for sequence analysis of the chromatograms, and ClustalW (http://www.genome.jp/tools/clustalw/) was used to compare the MoM envelope sequences to the reference CH040 or CH040-4013env sequence.

Experimental groups. The total number of experiments performed was determined on the basis of the total number of tissue cohorts (representing different human donors) and viral exposures used in each figure. For **Figure 1**, 12 human donors and 8 exposure groups are represented. For **Figure 2**, 13 human donors and 13 exposure groups are represented. For **Figure 3**, 5 human donors and 5 exposure groups are represented.

Statistical analyses. All data were graphed using GraphPad Prism (version 5.04). The statistical tests used are indicated in the figure legends and/or text for each comparison performed. All statistical tests were exact. A mixed-effects approach using Monolix (Lixoft, France), allowing for censored values, was used to model the decay slope for viremia after ART initiation, leading to an estimate for the half-life of productively infected cells in MoM and BLT mice. For half-life analyses, we assumed a near-perfect efficacy of the ART regimen to prevent new infections (>99%), yielding upper-bound estimates for half-lives. For comparisons in **Figure 2d**,**e** and **Supplementary Figure 3c**, a log-rank test was used, thus accounting for the variation in the lower limit of detection between samples similar to what has been done for other assays[37–39]. For all Mann–Whitney comparisons, a two-tailed test was used. For all comparisons, a P value <0.05 was considered statistically significant. No adjustment was made for multiple-hypothesis testing. No statistical methods were used to predetermine sample size. No randomization was used. Blinding of the statisticians (R.M.M. and Y.C.) was used when accessing and modeling the infected cell half-life following ART initiation (**Figs. 1c** and **2c**). Investigators were given viral loads for lettered groups of mice (A, B, C) but were not privy to the identity of the groups (MoM, ToM, or BLT mice) until all half-lives were calculated. No blinding was used for comparisons of the viral DNA and RNA levels of treated and untreated MoM (**Fig. 2d**,**e**).

Data availability. The sequencing data demonstrating point mutations in *env* for MoM 21 and MoM 23 were deposited in GenBank (accessions KX825880 and KX825881).

35. Strain, M.C. *et al.* Highly precise measurement of HIV DNA by droplet digital PCR. *PLoS One* **8**, e55943 (2013).
36. Honeycutt, J.B. *et al.* HIV-1 infection, response to treatment and establishment of viral latency in a novel humanized T cell–only mouse (TOM) model. *Retrovirology* **10**, 121 (2013).
37. Zhang, D., Fan, C., Zhang, J. & Zhang, C.H. Nonparametric methods for measurements below detection limit. *Stat. Med.* **28**, 700–715 (2009).
38. Lafleur, B. *et al.* Statistical methods for assays with limits of detection: serum bile acid as a differentiator between patients with normal colons, adenomas, and colorectal cancer. *J. Carcinog.* **10**, 12 (2011).
39. Gillespie, B.W. *et al.* Estimating population distributions when some data are below a limit of detection by using a reverse Kaplan–Meier estimator. *Epidemiology* **21** (Suppl. 4), S64–S70 (2010).

© 2017 Nature America, Inc., part of Springer Nature. All rights reserved.